DOI: 10.24352/UB.OVGU-2017-057 TECHNISCHE MECHANIK, 34, 3-4, (2014), 119 – 127
submitted: October 23, 2013

DEM Simulation of Concrete Fracture Phenomena

B. Beckmann, K. Schicktanz, M. Curbach

Concrete fracture phenomena are investigated in this work. It is the fracture processes and failure mechanisms which are specifically investigated rather than the reaching of a certain maximum load or the investigation of the concrete's behaviour within a range of safe working loads. The following questions are addressed. How do the crack positions vary from one test to another? Is it possible to identify in advance where for example micro-cracks will emerge to a global macro-crack later on? In order to investigate this matter, a two-dimensional numerical simulation based on the Discrete Element Method (DEM) is used for the analysis of concrete behaviour under compression load. Frictional behaviour, crack initiation and damage evolution are analysed. Regarding the concrete body, convex and concave geometries can be treated. The cracks are discrete just as in real laboratory experiments. The cracks arise due to the interaction of the concrete particle elements and without the predefinition of any crack zones or crack elements. The simulation results are compared to the ones of laboratory experiments. The ratio of longitudinal strain to lateral strain is obtained as a result of the simulation and compared to experimental results. The qualitative evolution of postprocessing entities such as stresses and strains is analysed.

1 Introduction

Concrete behaviour and concrete failure are numerically studied in this work. The primary aim is not to retrace the development of macroscopic quantities and to indicate a fracture upon the reaching a certain value of a macroscopic quantity such as stress or strain, but to let the fracture develop through the interaction of many simple entities, without an explicit inclusion of special macroscopic parameters or other additional degrees of freedom. In order to improve the comprehension of the interaction between microscopic and macroscopic phenomena during concrete failure, a two-dimensional discrete element simulation is used in this work. The failure procedure of regular cubic test specimens of 10 cm in length during a standard laboratory compression test is simulated and compared to laboratory experiments. In numerical simulations of concrete behaviour, the mechanical behaviour is transferred into a numerical model, i. e. according to Roelfstra et al. (1985) into "numerical concrete". Several experimental data concerning lightweight concrete, normal concrete, high-performance concrete (HPC) and ultra-high-performance concrete (UHPC) under biaxial and triaxial loads can be found in Curbach and Speck (2008), Speck and Curbach (2010), Scheerer and Curbach (2009) and Hampel et al. (2009), for example.

While the basic concept of DEM as well as several single aspects (e.g. contact approach) are taken from the literature, this work employs a combination of essential elements such as a contact approach including an overlap area, detection of new particle contacts during the simulation instead of neighbouring lists and particles with arbitrarily polygonal shape. For this reason, a two-dimensional simulation is used in this work. Khanal and Tomas (2010) notice that despite the lack of the third dimension, crack patterns of 2D simulations can be qualitatively compared to experimental results and that 2D simulations are justifiable from a comparison point of view.

Simulations of discrete particles are common in several research fields. In contrast to continuum-based methods, where the single elements result from a formal discretisation of an underlying continuum, in discrete methods the particles represent physical objects like grains in granular materials, molecules in biochemistry or stars in astrophysics, to give just a few examples. Some geometrical fundamentals like Voronoi tesselation and Delaunay triangulation can be found in continuum-based methods and in discrete methods alike and also in many other fields like computer graphics, crystallography and material sciences.

Originating from Cundall and Strack (1979), the Discrete Element Method (DEM) is a common approach. Several research groups use two-dimensional as well as three-dimensional DEM simulations for different applications such as granular material and bulk solids (Ghaboussi and Barbosa (1990), Kohring et al. (1995), Tillemans and Herrmann (1995), Saussine et al. (2006), Severens et al. (2006), Zhao et al. (2006), Khanal and Tomas (2008),

Walther and Sbalzarini (2009)), rock mechanics (Cundall (1988)), simulation of fracture processes (Diebels et al. (2001), D'Addetta and Ramm (2006), Ehlers et al. (2003), D'Addetta et al. (2004), Donzé et al. (2008), Rojek et al. (2012)). Some geometrical fundamentals are used in non-discrete models as well. Thus, spring networks and irregular lattice models are used for the simulation of cement mortar, cement composites and concrete (Landis and Bolander (2009), Bolander et al. (2008), Kim and Lim (2011)). An overview of DEM and of the coupling of the Discrete Element Method and the Finite Element Method can be found in Bicanic (2004). Hybrid and coupled methods are also described in the research group of Owen and Feng (Feng et al. (2010)).

Cundall and Hart (1992) point out two basic requirements for the description of discontinuous systems. The model must "(a) allow finite displacements and rotations of discrete bodies, including complete detachment, and (b) recognize new contacts automatically as the calculation progresses". Thus, one of the fundamental characteristics of particle simulations is that each particle can in principle interact with every other particle. This is an advantage and challenge at the same time. This means for example that two parts of the body that were not in contact or neighbouring at the beginning can make contact at a later time during the proceeding damage process of the concrete specimen. The capability of force transmission via new contacts arising during simulation is a presupposition for the modelling of slipping concrete parts that create new compressive contacts at other positions later on.

Contact detection is one of the essential parts of particle simulation due to the fact that new contacts have to be recognised. Cell-based (Griebel et al. (2004)) and tree-based approaches (Feng and Owen (2007)) as well as neighbouring lists (D'Addetta et al. (2002)) and separation algorithms (Chung Tat Leung (1996), Nezami et al. (2004), Muth et al. (2007)) are used in the literature. In spring networks, no contact detection is used, since the contact is modelled by springs between neighbouring particles. Existing contacts between particles can break during simulation, but new particle contacts are not detected and are not part of the simulation method in spring networks.

Investigating concrete failure patterns and crack initiation, discontinuities in deformation and displacement are in focus. Within the DEM simulation, discontinuities are an inherent part of the simulation method. For the evolution of cracks no additional descriptions like special crack elements are required. The disruption of linkages between particles automatically initiates a macroscopic crack pattern. For this reason, DEM simulations are especially favourable for investigating crack initiation and fracture processes. Plassiard and Donzé (2009) notice that slipping surfaces and collapse processes can be described by particle methods due to their explicitly discrete nature.

2 Mechanical Model

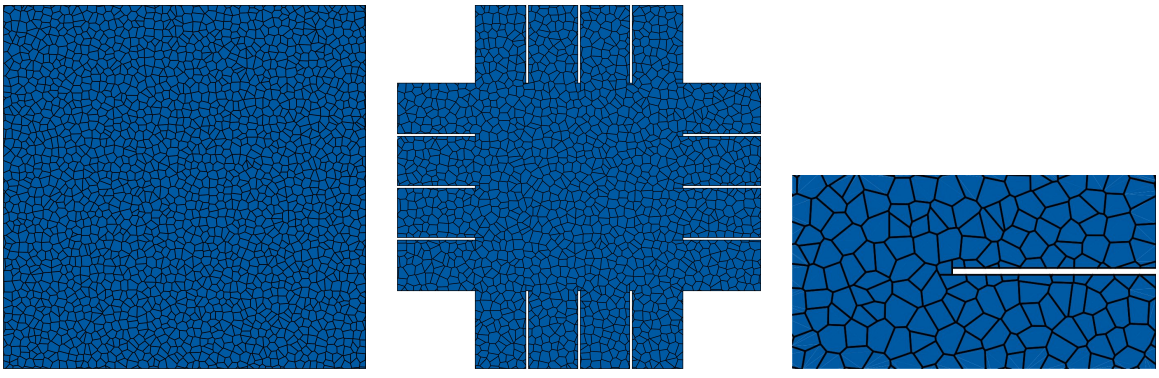

(a) (b) (c)

Figure 1: Convex (a) and non-convex (b, c) boundaries of the concrete object

Using the principles of classical mechanics and especially Newton's equations, the acceleration of each single particle depends on the force acting on it, e. g. Griebel et al. (2004). For each particle p the equation of motion is given by

$$m_{ij}^p \, \ddot{x}_j^p = F_i^p. \tag{1}$$

In a two-dimensional simulation with translations in the x- and y-directions and a rotation around the z-axis, this means

$$\begin{bmatrix} m^p & 0 & 0 \\ 0 & m^p & 0 \\ 0 & 0 & \theta^p \end{bmatrix} \cdot \begin{bmatrix} \ddot{x}^p \\ \ddot{y}^p \\ \ddot{\varphi}^p \end{bmatrix} = \begin{bmatrix} F_x^p \\ F_y^p \\ M_z^p \end{bmatrix} \tag{2}$$

where m^p is the mass of a particle p and θ^p the polar moment of inertia.

The forces result from the interaction with the other particles and depend on their positions, velocities and masses. The force acting on a particle p consists of an external force like gravity, the particle contact force and an optional cohesive bonding force

$$F_i^p \;=\; {}^{ext}F_i^p + {}^{c}F_i^p + {}^{b}F_i^p = \; {}^{ext}F_i^p + \sum_q {}^{c}F_i^{pq} \; + \sum_s {}^{b}F_i^{ps} \tag{3}$$

where the contact forces of particle p with all colliding particles q are summed up as well as all bonding forces connecting particle p with all particles s.

In the presented work, the interaction force is calculated using a particle contact approach following Kohring et al. (1995), Tillemans and Herrmann (1995) and D'Addetta et al. (2002) where the repulsive normal force ${}^{c}F_i^{pq,n}$ and the repulsive tangential force ${}^{c}F_i^{pq,t}$ are given by

$${}^{c}F_i^{pq,n} = \frac{1}{\ell}\, kA^{pq} d\; n_i \;-\; m^{red}\gamma^n v^{rel,n} n_i, \qquad {}^{c}F_i^{pq,t} = -\operatorname{sign}(v^{rel,t})\; \min\left(m^{red}\,\gamma^t \left|v^{rel,t}\right|,\; \mu\,|{}^{c}\mathbf{F}^{pq,n}|\right)\; t_i. \tag{4}$$

An assumed overlap area A^{pq} of two colliding particles p and q with the material-specific stiffness k and the (constant) thickness d leads to a repulsive force which reduces the overlap area in the next step. The term $\frac{1}{\ell}$ refers to the characteristic contact length following D'Addetta et al. (2002). The dissipation term $m^{red}\gamma^n v^{rel,n} n_i$ as well as the frictional tangential force ${}^{c}F_i^{pq,t}$ are taken from Kohring et al. (1995).

A convex particle shape is necessary to avoid multipiece overlap areas. Apart from that, a convex particle shape simplifies the calculation of the overlap area. Convex particles and therefore convex overlap areas can be determined by clipping algorithms as shown in Fellner (1992). During the contact force calculation, the point where the contact force due to interpenetration of two particles is applied is in principle arbitrarily settable within the overlap area. Here, it is set at the midpoint of the intersection line as described in D'Addetta et al. (2002).

In addition to the contact force due to the overlap area, an optional lattice of bars is employed, providing the simulation of cohesion and tensile force. For the calculation of the bar forces, the equations of classical elastic framework bars (or optionally also beams) are used. A bar breaks and is taken away from the simulation when a maximum elongation of the bar based on a maximum strain $\varepsilon^{max} = 0.003$ is reached. In contrast to the contact forces where new contacts can occur at any time during the simulation, the bonding bars are generated just once at the beginning of the simulation.

For the contact detection, a multilevel algorithm is used in this work. At the first and most efficient level, Linked Cells following Griebel et al. (2004) are used. Furthermore, the distance of two particles compared with their sizes, the Separated Vector Algorithm following Chung Tat Leung (1996) and the interdependency of the collision of particle p with q and particle q with p are used for contact detection and reduction of numerical effort, respectively.

To simulate the evolution of the assembly of interacting particles, the equation of motion is integrated for each particle. There is no need to solve a system of partial differential equations (PDE), but only decoupled ordinary differential equations (ODE), which is favourable from the numerical point of view. For the time integration, a velocity Störmer–Verlet algorithm (e. g. Griebel et al. (2004)) is used.

For the particle representation, i. e. the particle geometry, the Vectorizable Random Lattice (VRL) algorithm of Moukarzel and Herrmann (1992) is used. This approach using arbitrary polygons is especially suitable for the modelling of concrete behaviour. Convex geometries of the concrete object can be treated with no further ado (Figure 1a). To simulate concave shapes of the whole concrete body (Figure 1b), as found in the work of Jesse and Jesse (2009) for example, the particle generation procedure is refined and a special particle trim algorithm is introduced. If the boundary of the object is non-convex, those particles which are located in a concave section of the boundary are divided into several convex sub-particles (Figure 1c). In doing so, the necessary convexity of the particles themselves is preserved.

Macroscopically relevant average quantities such as stresses and strains are determined in a postprocessing procedure. The averaging approach follows Hill (1963) and is particularly discussed in D'Addetta et al. (2004). Note that stresses and strains are not state variables and, therefore, do not influence the actual simulation.

For the calculation of stresses and strains, a representative volume element (RVE) is specified. Within the RVE, the stress and strain are assumed to be constant. In Figure 2, radius r of the RVE, i. e. the extent of the average region,

is chosen as approximately four times the particle size. Calculating the stresses and strains for a certain particle p, all particles a located at the boundary of the average region are needed. Due to the motion of the particles, a new particle configuration can occur during the simulation. Therefore, the detection of the particles a is renewed for each calculation. For a correct stress and strain calculation, a closed average region (i. e. a closed circle in Figure 2) is required. For this reason, no stresses and strains can be calculated for particles located at the boundary of the concrete body.

The stress σ_{ij} of a particle p is given by

$$\langle \sigma_{ij} \rangle^p = \frac{1}{2\pi r^2 d} \sum_a x_i^a f_j^a \tag{5}$$

where x_i^a are the positions and f_j^a the forces of the particles a; r is the chosen radius of the average region, and d is the (constant) thickness of the concrete body. The strain ε_{ij} of a particle p is given by

$$\langle \varepsilon_{ij} \rangle^p = \frac{d}{2\pi r^2 d} \sum_a (n_j^a u_i^a + n_i^a u_j^a)\, \ell^a \tag{6}$$

where u_i^a are the displacements of the particles a, n_j is the unit outward normal (Hill (1963)), and ℓ^a is the length of the particles a on the boundary of the average region. Equations 5 and 6 follow from the assumed constancy of the stress and strain within the RVE.

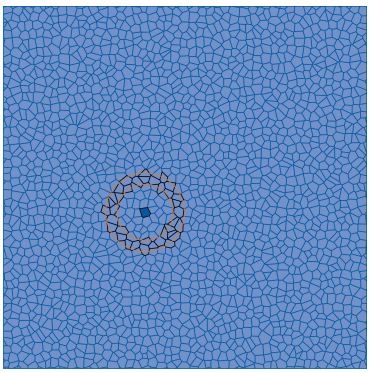

Figure 2: Particles on the boundary of the average region

The calculation of stresses and strains can formally be performed at every loading state. But it is only meaningful for undamaged or barely damaged specimens. With proceeding crack evolution and with increasing damage, the necessary presupposition of continuous fields is no longer given.

3 Simulation Results

3.1 Crack Patterns

The crack evolution and the failure process during the standard laboratory compression test of concrete specimens are simulated. The cubic concrete specimen of 10 cm length is loaded up to total collapse. The load is applied velocity controlled with a velocity of the (upper) loading plate of 0.1 m/s and with no displacement of the (lower) load-bearing plate. In reality, two test specimens are never absolutely equal, even if they are produced from the same charge and tested under the same conditions. The measured values of the compression strength within a series of three test specimens usually vary by a few percent. The crack patterns are phenomenologically similar, but the exact positions of the cracks and of the spalling disperse and are never exactly identical. This statistical characteristic can be seen in the simulation results as well. Two simulations are shown in Figures 3a and 3b, where all simulation parameters are held constant and the only alteration is due to the slightly varying particle numbers (5 092 and 5 076 particles, this means a particle size of approximately 1.4 mm) and hence the varying individual particle positions. It can be seen that – as in real laboratory experiments – the crack patterns are phenomenologically similar, but differ in details. It is shown in Beckmann et al. (2012) that the number of particles used does not influence the calculated break load.

(a) (b)

Figure 3: Crack patterns and failure of the concrete specimen in the DEM simulation

3.2 Damage Evolution

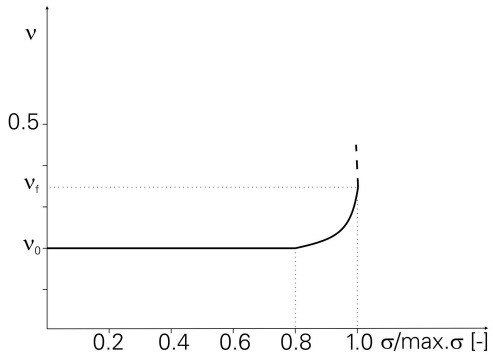

(a) Ratio of lateral strain to longitudinal strain according to Schlüter (1987)

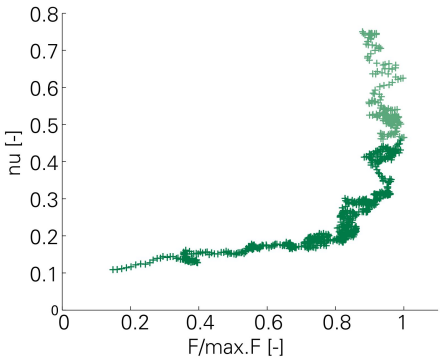

(b) Ratio of lateral to longitudinal strain in the DEM simulation

Figure 4: Ratio of lateral to longitudinal strain related to the load

The question of how the lateral strain evolves related to the longitudinal strain during the loading process is of special interest in concrete engineering. Note that the Poisson's ratio in the sense of elastic continuum mechanics is not the issue in this context here. However, the ratio of lateral and longitudinal strain during the load application is investigated separate from the assumptions of the elastic theory. Schlüter (1987) shows that the ratio of lateral strain to longitudinal strain is constant up to a load of about 80% of the ultimate load and severely increases above this load intensity (Figure 4a). Figure 4b shows the ratio of lateral to longitudinal strain calculated in the DEM simulation. The ratio of lateral to longitudinal strain is not a simulation parameter, but a postprocessing value calculated referring to particle positions. Comparing both figures, the simulated results agree with the experimental results. Above a critical load intensity the ratio of lateral and longitudinal strain increases strongly (and above the limit known from elastic theory). This indicates that the concrete body is no longer a continuous body due to the increasing crack propagation and the severe damage evolution.

The proceeding damage evolution can be seen in Figure 5, too. Since tension and cohesive forces can only be transmitted via the elements of the bar lattice, the number of broken bars, i. e. the number of disrupted tension linkages, can be regarded as an indicator of the degree of damage. It is shown that a disproportionate number of tension linkages break at a high damage intensity. The increasing damage accumulation is shown by Rojek et al. (2013), too.

3.3 Stresses and Strains

The distribution of the vertical stress σ_{yy} is shown in Figure 6 for different loading states. Figure 6a shows the stress at maximum load intensity, Figure 6b during post-peak behaviour and Figure 6c at almost total collapse. In

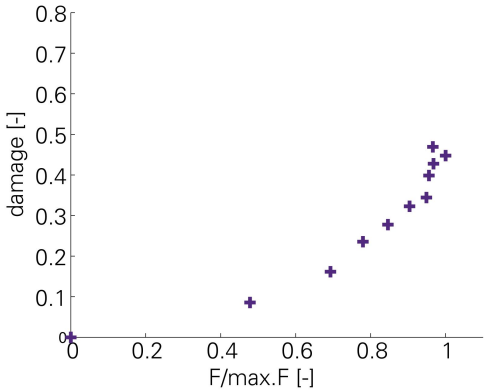

Figure 5: Damage accumulation

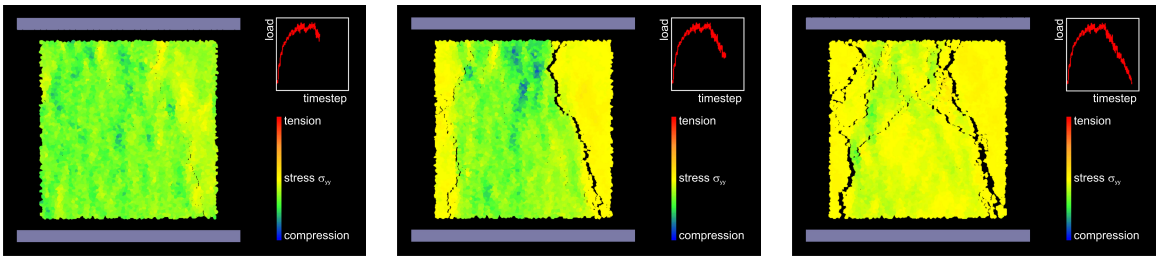

(a) (b) (c)

Figure 6: Stress evolution

the yellow-coloured regions, hardly any or no stress is transmitted. Further spalling can be seen, before macro-cracks entirely arise (Figure 6a). The evolution of the horizontal strain ε_{xx} is shown in Figure 7. During the loading increase (Figures 7a and 7b), regions of higher strain can be seen, where macro-cracks will appear during further loading progression. As already mentioned above, the strain calculation in post-peak behaviour (and even more so at total collapse) can formally be done, but it is not meaningful at these loading states. The strain shown in Figure 7c can be interpreted as an indication of increasing crack evolution and severe damage rather than a certain value of strain. The calculation of stresses and strains presupposes a continuous body and continuous fields. This is not the case where a large amount of damage has occurred. This relation can be found in Figures 4 and 5 as well. All the figures show that the concrete body is no longer a continuous body at further loading states.

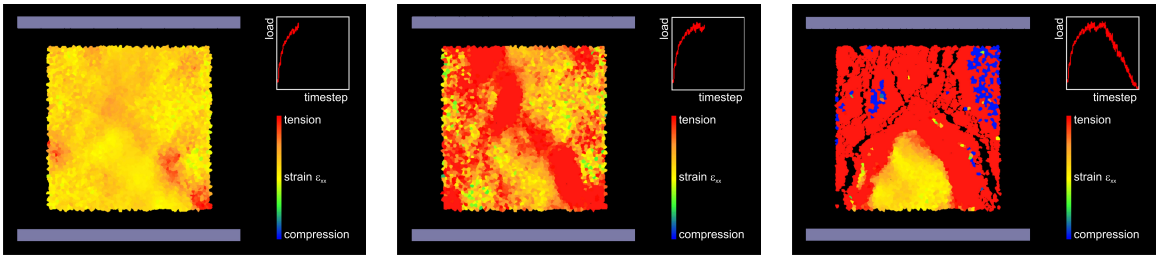

(a) (b) (c)

Figure 7: Strain evolution

4 Concluding Remarks

A two-dimensional simulation of concrete failure processes and crack propagation using discrete elements is presented in this work. A special advantage of the Discrete Element Method is that discontinuities are an inherent property of the method. Thus cracks do not need to be additionally included with any special crack elements, but are a discontinuous feature and part of the method a priori. Using many simple particles, macroscopically observable effects emerge due only to the interaction of the particles, and an explicit inclusion of macroscopic parameters is avoided. Simulated crack patterns of concrete specimens subjected to standard compression test are

shown and compared to the ones of real laboratory tests. Being of special interest in concrete engineering, the ratio of lateral to longitudinal strain is analysed in the DEM simulation and compared to experimental results. In agreement with real experiments, the simulation shows that the ratio of lateral to longitudinal strain increases strongly above approximately 80% load intensity. At this state, the concrete specimen can no longer be seen as a continuous body due to increased crack evolution and proceeding damage accumulation. Along with this, the assumption of a continuous concrete body and of continuous fields becomes invalid. As a consequence it is found that the calculation of stresses and strains is meaningful only at low loading states. The presented results and crack patterns show that a DEM simulation is a suitable approach for the numerical investigation of concrete behaviour and crack propagation.

References

Beckmann, B.; Schicktanz, K.; Reischl, D.; Curbach, M.: Dem simulation of concrete fracture and crack evolution. *Structural Concrete*, 13, 4, (2012), 213–220.

Bicanic, N.: *Encyclopedia of Computational Mechanics*, vol. 1: Fundamentals, chap. 11 Discrete Element Methods, pages 311–337. John Wiley & Sons (2004).

Bolander, J.; Choi, S.; Duddukuri, S.: Fracture of fiber-reinforced cement composites: effects of fiber dispersion. *International Journal of Fracture*, 154, (2008), 73–86.

Chung Tat Leung, K.: *An Efficient Collision Detection Algorithm for Polytopes in Virtual Environments*. Master's thesis, University of Hong Kong (1996).

Cundall, P.: Formulation of a three-dimensional distinct element model–part i. a scheme to detect and represent contacts in a system composed of many polyhedral blocks. *International Journal of Rock Mechanics and Mining Sciences & Geomechanics Abstracts*, 25, 3, (1988), 107–116.

Cundall, P. A.; Hart, R. D.: Numerical modelling of discontinua. *Engineering Computations*, 9, (1992), 101–113.

Cundall, P. A.; Strack, O. D. L.: A discrete numerical model for granular assemblies. *Géotechnique*, 29, (1979), 47–65.

Curbach, M.; Speck, K.: Ultra high performance concrete under biaxial compression. In: *Schriftenreihe Baustoffe und Massivbau*, vol. 10, pages 477–484 (2008).

D'Addetta, G.; Ramm, E.: A microstructure-based simulation environment on the basis of an interface enhanced particle model. *Granular Matter*, 8, 3/4, (2006), 159 – 174.

D'Addetta, G. A.; Kun, F.; Ramm, E.: On the application of a discrete model to the fracture process of cohesive granular materials. *Granular Matter*, 4, 2, (2002), 77–90.

D'Addetta, G. A.; Ramm, E.; Diebels, S.; Ehlers, W.: A particle center based homogenization strategy for granular assemblies. *Engineering Computations*, 21, (2004), 360–383.

Diebels, S.; Ehlers, W.; Michelitsch, T.: Particle simulations as a microscopic approach to a cosserat continuum. *J. Phys. IV France*, 11, 5, (2001), 203–210.

Donzé, F. V.; Richefeu, V.; Magnier, S.-A.: Advances in discrete element method applied to soil, rock and concrete mechanics. *EJGE*, (2008).

Ehlers, W.; Ramm, E.; Diebels, S.; D'Addetta, G. A.: From particle ensembles to Cosserat continua: homogenization of contact forces towards stresses and couple stresses. *International Journal of Solids and Structures*, 40, 24, (2003), 6681–6702.

Fellner, W.-D.: *Computergrafik*. BI-Wissenschaftsverlag (1992).

Feng, K. H. A. Y. T.; Owen, D. R. J.: Performance comparisons of tree-based and cell-based contact detection algorithms. *Engineering Computations: International Journal for Computer-Aided Engineering and Software*, 24, 2, (2007), 165–181.

Feng, Y. T.; Han, K.; Owen, D. R. J.: Combined three-dimensional lattice Boltzmann method and discrete element method for modelling fluid-particle interactions with experimental assessment. *Int. J. Numer. Meth. Engng*, 81, (2010), 229–245.

Ghaboussi, J.; Barbosa, R.: Three-dimensional discrete element method for granular materials. *International Journal for Numerical and Analytical Methods in Geomechanics*, 14, (1990), 451–472.

Griebel, M.; Knapek, S.; Zumbusch, G.; Caglar, A.: *Numerische Simulation in der Molekldynamik: Numerik, Algorithmen, Parallelisierung, Anwendungen*. Springer-Lehrbuch, Springer Verlag, Berlin (2004).

Hampel, T.; Speck, K.; Scheerer, S.; Ritter, R.; Curbach, M.: High performance concrete under biaxial and triaxial loads. *ASCE Journal of Engineering Mechanics*, 135, 11, (2009), 1274–1280.

Hill, R.: Elastic properties of reinforced solids: Some theoretical principles. *J. Mech. Phys. Solids*, 11, (1963), 357–372.

Jesse, D.; Jesse, F.: Tragverhalten von Textilbeton unter zweiaxialer Zugbeanspruchung. In: M. Curbach; F. Jesse, eds., *Textile Reinforced Structures : Proceedings of the 4th Colloquium on Textile Reinforced Structures (CTRS4) und zur 1. Anwendertagung, Dresden, 3.-5.6.2009. SFB 528, Technische Universität Dresden*, pages 129–144, Eigenverlag (2009).

Khanal, M.; Tomas, J.: Interparticle collision of particle compositesfinite and discrete element simulations. *Particulate Science & Technology*, 26, 5, (2008), 460 – 466.

Khanal, M.; Tomas, J.: Application of dem to evaluate and compare process parameters for a particle failure under different loading conditions. *Granular Matter*, 12, 4, (2010), 411 – 416.

Kim, K.; Lim, Y. M.: Simulation of rate dependent fracture in concrete using an irregular lattice model. *Cement and Concrete Composites*, 33, 9, (2011), 949 – 955.

Kohring, G. A.; Melin, S.; Puhl, H.; Tillemans, H.; Vermhlen, W.: Computer simulations of critical, non-stationary granular flow through a hopper. *Computer Methods in Applied Mechanics and Engineering*, 124, (1995), 273–281.

Landis, E. N.; Bolander, J. E.: Explicit representation of physical processes in concrete fracture. *Journal of Physics D: Applied Physics*, 42, 21, (2009), 214002.

Moukarzel, C.; Herrmann, H. J.: A vectorizable random lattice. *J. Stat. Phys.*, 68, (1992), 911–923.

Muth, B.; Of, G.; Eberhard, P.; Steinbach, O.: Collision detection for complicated polyhedra using the fast multipole method or ray crossing. *Arch Appl Mech*, 77, (2007), 503–521.

Nezami, E. G.; Hashash, Y. M.; Zhao, D.; Ghaboussi, J.: A fast contact detection algorithm for 3-d discrete element method. *Computers and Geotechnics*, 31, 7, (2004), 575 – 587.

Plassiard, J.-P.; Donzé, F.-V.: Rockfall impact parameters on embankments: A discrete element method analysis. *Structural Engineering International*, 19, 3, (2009), 333–341.

Roelfstra, P. E.; Sadouki, H.; Wittmann, F. H.: Le béton numérique. *Materials and Structures*, 18, (1985), 327–335.

Rojek, J.; Labra, C.; Marczewska, I.: Influence of parameter evaluation on failure mode in discrete element models for rock materials. In: P. Dluzewski; G. Jurczak; T. D. Young, eds., *ICMM3 - 3rd International Conference on Material Modelling*, Warsaw, Poland (September 8-11, 2013).

Rojek, J.; Labra, C.; Su, O.; Oate, E.: Comparative study of different discrete element models and evaluation of equivalent micromechanical parameters. *International Journal of Solids and Structures*, 49, 13, (2012), 1497 – 1517.

Saussine, G.; Cholet, C.; Gautier, P.; Dubois, F.; Bohatier, C.; Moreau, J.: Modelling ballast behaviour under dynamic loading. part 1: A 2d polygonal discrete element method approach. *Computer Methods in Applied Mechanics and Engineering*, 195, 19-22, (2006), 2841 – 2859.

Scheerer, S.; Curbach, M.: Structural engineering. In: H.-J. Bullinger, ed., *Technology Guide. Principles - Applications - Trends*, pages 426–431, Springer, Berlin (2009).

Schlüter, F.-H.: *Dicke Stahlbetonplatten unter stoßartiger Belastung – Flugzeugabsturz –*. Ph.D. thesis, Universität Fridericiana zu Karlsruhe (TH) (1987).

Severens, I. E. M.; van de Ven, A. A. F.; Wolf, D. E.; Mattheij, R. M. M.: Discrete element method simulations of toner behavior in the development nip of the oc direct imaging print process. *Granular Matter*, 8, (2006), 137–150.

Speck, K.; Curbach, M.: Fracture criterion for all concretes – normal, lightweight, high- and ultrahigh-performance concrete. In: *3rd International fib Congress, Washington, D.C.* (2010).

Tillemans, H.-J.; Herrmann, H. J.: Simulating deformations of granular solids under shear. *Physica A: Statistical and Theoretical Physics*, 217, (1995), 261–288.

Walther, J. H.; Sbalzarini, I. F.: Large-scale parallel discrete element simulations of granular flow. *International Journal for Computer-Aided Engineering and Software*, 26, (2009), 688–697.

Zhao, D.; Nezami, E. G.; Hashash, Y. M.; Ghaboussi, J.: Three-dimensional discrete element simulation for granular materials. *International Journal for Computer-Aided Engineering and Software*, 23, 7, (2006), 749–770.

Address: Institute of Concrete Structures, TU Dresden, George-Bähr-Str. 1, 01069 Dresden, Germany
email: `Birgit.Beckmann@tu-dresden.de`